Mismatch Effects in Time-Interleaved Oversampling Converters

Ramin Khoini-Poorfard
Dept. of Electrical and Computer Engineering
University of Toronto
Toronto, Ont., M5S 1A1, CANADA
ramin@eecg.toronto.edu

David A. Johns
Dept. of Electrical and Computer Engineering
University of Toronto
Toronto, Ont., M5S 1A1, CANADA
johns@eecg.toronto.edu

ABSTRACT

Recently, a new architecture was proposed which utilizes the concept of time-interleaving in oversampling converters. Using this architecture, one is theoretically able to achieve higher resolutions by using an array of interconnected modulators without increasing the oversampling ratio or order of the modulators. Alternatively, the same resolution can be maintained with wider bandwidth input signals. This paper presents the first experimental results on this new family of modulators. As well, the practical issue of component mismatch for these converters are studied and some suggestions are made to alleviate the effects of this problem.

I. INTRODUCTION

The speed and resolution of data converters are of utmost importance in mixed digital-analog applications. The emergence of new applications, such as HDTV, accelerates the need for the implementation of high-speed and high-resolution converters. In the area of high speed converters, Nyquist rate designs are the popular choice whereas in the high-resolution domain, oversampling modulators are the most favorable ones. Up to now, the latter one, due to the nature of oversampling, is suitable for lower speed applications such as digital audio.

To realize faster oversampling converters, a new architecture was recently proposed where the idea of time-interleaving was exploited [1]. The time-interleaving concept was proposed for Nyquist-rate converters in the early 80's [2]. In this paper, time-interleaved oversampling modulators are studied from a practical point of view. Specifically, the practical issue of performance deterioration due to component mismatch is considered in detail.

The paper organization is as follows. In section 2, the theoretical background of time-interleaved oversampling converters is presented. Section 3 covers an illustrative example as well as experimental results for a second-order time-interleaved D/A converter. In section 4, the problem of component mismatch and its effect on aliasing is addressed. Also, methods for reducing the amount of aliasing due to component mismatch are briefly discussed. Finally, conclusions are given in section 5.

II. TIME-INTERLEAVED ARCHITECTURE

A time-interleaved structure is basically a multi-rate system in which parallelism is exploited to reduce the speed requirement on each processing element. Consider the following single-input single-output transfer function $Y(z) = H(z)X(z)$. An equivalent system with the same input-output transfer function is depicted in Fig. 1, in which $\overline{H}(z)$ is an $M \times M$ transfer function matrix, where $\overline{H}_{ij}$ represents the contribution of the j'th input into the i'th output. The general structure of $\overline{H}(z)$ is as follows,

$$\overline{H}(z) = \begin{bmatrix} E_0(z) & E_1(z) & E_2(z) & \dots & E_{M-1}(z) \\ z^{-1}E_{M-1}(z) & E_0(z) & E_1(z) & \dots & E_{M-2}(z) \\ z^{-1}E_{M-2}(z) & z^{-1}E_{M-1}(z) & E_0(z) & \dots & E_{M-3}(z) \\ \vdots & \vdots & \vdots & \vdots & \vdots \\ z^{-1}E_1(z) & z^{-1}E_2(z) & z^{-1}E_3(z) & \dots & E_0(z) \end{bmatrix} \quad (1)$$

in which the elements of the first row of $\overline{H}(z)$ are type 1 poly-phase components of $H(z)$, or mathematically,

$$H(z) = \sum_{l=0}^{M-1} z^{-l} E_l(z^M) \quad (2)$$

The above realization is referred to as block digital filtering [3]. Now consider the general interpolative $\Delta\Sigma$ architecture as shown in Fig. 2(a). Using the equivalent block digital filter $\overline{H}_i(z)$ instead of $H_i(z)$ and applying several topological identities on the structure (using a linear model for the quantizer), one derives the proposed architecture shown in Fig. 2(b). Note that the proposed structure is in fact a multi-rate nonlinear system and as far as authors are aware this is the first reported application of such a system. Also note that, the same procedure is applicable to other $\Delta\Sigma$ structures such as error-feedback or cascade-of-integrators topologies. In fact in [1], simulation results were given for a second-order modulator based on cascade of integrators topology.

III. Illustrative Example and Experimental Results

We illustrate the design procedure of a second-order time-interleaved D/A in this section. An error-feedback topology as depicted in Fig. 3(a) is chosen for this purpose. The feedback transfer function is $H(z) = -2z^{-1} + z^{-2}$. Assuming a time-interleaving factor of two (i.e. $M = 2$), one has the following polyphase components for $H(z)$: $E_0(z) = z^{-1}$ and $E_1(z) = -2$. Hence,

$$\overline{H}(z) = \begin{bmatrix} z^{-1} & -2 \\ -2z^{-1} & z^{-1} \end{bmatrix} \quad (3)$$

Based on the derived $\bar{H}(z)$, the equivalent time-interleaved structure is derived and shown in Fig. 3(b). This architecture was implemented on an FPGA chip and tested with the following experimental setup. A DAT machine generates a 1 kHz 16 bit digital signal sampled at 44.1 kHz. The data is interpolated 8 times by a simple zero-order hold which is interleaved by two in the case of a time-interleaved modulator. Hence the final clocks for the conventional and time-interleaved modulators are 352.8 kHz and 176.2 kHz respectively. It is also worth mentioning that the interpolator section can be designed in a time-interleaved fashion as well, resulting in the clocking frequency in the interpolation portion of time-interleaved modulator also being 176.2 kHz (Fig. 3(b)). In fact, the only circuitry clocked at 352.8 kHz is the final demultiplexor bringing the two outputs back into one bitstream.

To make a fair comparison, a conventional second-order modulator was also tested. Fig. 4 shows the output spectrums of the two designs when both are clocked at the same rate. Here, one can see that the time-interleaved modulator has 15dB better SNR as expected by theory. In fact the two parallel modulators inside a time-interleaved structure work as one modulator clocked at twice the rate.

IV. Mismatch Analysis of Block Digital Filtering

Block digital filtering is based on perfect aliasing cancellation. Therefore, any deviation of $\bar{H}_{ij}$'s from their ideal values is reflected into aliasing generation. Such deviations could be due to coefficient mismatches if the block filter is built with analog components (i.e. SC filters). Thus an architecture based on block digital filters, such as time-interleaved $\Delta\Sigma$ converters, would also have the same problem. For example, in a time-interleaved $\Delta\Sigma$ A/D converter, the SC modulator block will incur some mismatching whereas the digital decimation block would be mismatch free. Conversly, in a time-interleaved $\Delta\Sigma$ D/A converter, the digital modulator behaves ideally whereas the analog post-filtering block will suffer from mismatching. In this section an attempt has been made to compute the effect of mismatching on the overall performance of a block digital filter.

Consider Fig. 1 again. The input-output relation is as follows.

$$Y(z) = \frac{1}{M}\sum_{l=0}^{M-1} X(zW^l)\sum_{k=0}^{M-1} W^{-lk}\sum_{s=0}^{M-1} z^{-k}z^{-(M-1-s)}h_{s,k}(z^M) \quad (4)$$

where $W = e^{-\frac{j2\pi}{M}}$. Using the following notations,

$$\bar{X}(z) = [X(z), X(zW), \ldots, X(zW^{M-1})] \quad (5)$$

$$\bar{W} = [W^{-lk}]_{k=0,\ldots,M-1}^{l=0,\ldots,M-1} \quad (6)$$

$$\bar{V}^t = [V_0(z), V_1(z), \ldots, V_{M-1}(z)], \quad (7)$$

$$\bar{\Lambda}(z) = \frac{\overline{W^\dagger}\,\bar{V}(z)}{M} \quad (8)$$

where $V_k(z) = \sum_{s=0}^{M-1} z^{-k}z^{-(M-1-s)}h_{s,k}(z^M)$, and $\overline{W^\dagger}$ is complex conjugate of $\bar{W}$, one can rewrite (4) in its matrix form as

$$Y(z) = \bar{X}(z)\bar{\Lambda}(z) \quad (9)$$

If there is no mismatch then,

$$\bar{\Lambda}^t = [H(z), 0, \ldots, 0] \quad (10)$$

and hence, $Y(z) = X(z)H(z)$.

However, in presence of mismatch one can write,

$$h_{s,k}(z) = h^i_{s,k}(z) + \Delta h_{s,k}(z) \quad (11)$$

where $h^i_{s,k}(z)$ is the ideal term and $\Delta h_{s,k}(z)$ is the error term. Inserting (11) into (4), we have

$$Y(z) = X(z)H(z) + \bar{X}(z)\overline{\Delta\Lambda}(z) \quad (12)$$

in which, $\overline{\Delta\Lambda}(z) = \frac{\overline{W^\dagger}\,\overline{\Delta V}(z)}{M}$ and

$$\Delta V_k(z) = \sum_{s=0}^{M-1} z^{-k}z^{-(M-1-s)}\Delta h_{s,k}(z^M) \quad (13)$$

$$\Delta\Lambda_l(z) = \frac{1}{M}\sum_{k=0}^{M-1} W^{-lk}\Delta V_k(z) \quad (14)$$

Hence, the input-output relation can be written as

$$Y(z) = (H(z) + \Delta\Lambda_0(z))X(z) + L(z) \quad (15)$$

where, $L(z) = \sum_{l=1}^{M-1} X(zW^l)\Delta\Lambda_l(z)$ are the aliasing terms. In other words, aliased versions of the input spectrum ($X(zW^l)$'s) will first get attenuated by $\Delta\Lambda_l(z)$ and then fold back into the band of interest. Hence, it is important to study $\Delta\Lambda_l(z)$ more thoroughly. While equation (15) is in its most general form, more insightful results can be driven for a special case where $H(z)$ is an FIR filter. In this case, $\Delta h_{s,k}(z^M) = \sum_{n=0}^{N_{s,k}-1} a_{s,k,n}h^i_{s,k,n}z^{-n}$ where $N_{s,k}$ is the order of each FIR term in $\bar{H}(z)$, $a_{s,k,n}$'s are the mismatch ratios and $h^i_{s,k,n}$'s are the ideal coefficients. Hence,

$$\Delta\Lambda_l(z) = \frac{1}{M}\sum_{k=0}^{M-1} W^{-lk}z^{-k}\sum_{s=0}^{M-1} z^{-(M-1-s)}\sum_{n=0}^{N_{s,k}-1} a_{s,k,n}h^i_{s,k,n}z^{-n} \quad (16)$$

In the context of low-pass oversampling converters only the amount of aliasing around DC is important. Hence, the characteristic of $\Delta\Lambda_l(z)$ is only important around DC or $z = 1$. Therefore, we focus our study on $\Delta\Lambda_l(1)$ which is

$$\Delta\Lambda_l(1) = \frac{1}{M}\sum_{k=0}^{M-1} W^{-lk}\sum_{s=0}^{M-1}\sum_{n=0}^{N_{s,k}-1} a_{s,k,n}h^i_{s,k,n} \quad (17)$$

Knowing that $a_{s,k,n}$'s (mismatch ratios) are random variables, one can conclude that $|\Delta\Lambda_l(1)|$'s are random variables too. Recall that $|\Delta\Lambda_l(1)|$ is the amount of attenuation applied to the input spectrum before being folded back into the band of interest around DC. Hence, $|\Delta\Lambda_l(1)|$ is a good gauge for performance deterioration of a block digital structure due to mismatching. In fact the following corollaries help one to determine the expected and worst-case values of $|\Delta\Lambda_l(1)|$ after building a block digital

structure such as a time-interleaved oversampling converter in the presence of mismatching.

Corollary 1: If mismatch ratios ($a_{s,k,n}$'s) are independent, zero mean and have $E(a_{s,k,n}^2) = \sigma_a^2$, then $\Delta\Lambda_l(1)$'s are zero mean, independent, and have

$$E(|\Delta\Lambda_l(1)|^2) = \frac{\sigma_a^2 M}{M} \sum_{s=0}^{M-1} \sum_{n=0}^{N_{s,k}-1} (h_{s,k,n}^i)^2 \tag{18}$$

Proof: Only the proof for second part is given here. The proof for $\Delta\Lambda_l(1)$ being zero mean is straightforward.

$$E(\Delta\Lambda_l(1)\Delta\Lambda_{l'}^*(1)) = \frac{1}{M^2} \sum_{k=0}^{M-1} \sum_{k'=0}^{M-1} W^{-(lk+l'k')} \sum_{s=0}^{M-1} \sum_{s'=0}^{M-1} \sum_{n=0}^{N_{s,k}-1} \sum_{n'=0}^{N_{s',k'}-1} E(a_{s,k,n} a_{s',k',n'}) h_{s,k,n}^i h_{s',k',n'}^i \tag{19}$$

Knowing that $a_{s,k,n}$'s are independent we conclude:

$$E(\Delta\Lambda_l(1)\Delta\Lambda_{l'}^*(1)) = \frac{\sigma_a^2 M}{M} \sum_{k=0}^{M-1} W^{-k(l-l')} \sum_{s=0}^{M-1} \sum_{n=0}^{N_{s,k}-1} (h_{s,k,n}^i)^2 \tag{20}$$

in which $\sum_{s=0}^{M-1} \sum_{n=0}^{N_{s,k}-1} (h_{s,k,n}^i)^2$ is the square summation of all the coefficients of row number k of $\overline{H}(z)$. This double summation is independent of k due to pseudocirculant nature of $\overline{H}(z)$. Hence, we conclude

$$E(\Delta\Lambda_l(1)\Delta\Lambda_{l'}^*(1)) = \begin{cases} \frac{\sigma_a^2 M}{M} \sum_{s=0}^{M-1} \sum_{n=0}^{N_{s,k}-1} (h_{s,k,n}^i)^2 & l = l' \\ 0 & \text{otherwise} \end{cases} \tag{21}$$

Corollary 2: If $a_{s,k,n} \in [-A, A]$ and M is even, then

$$\text{Max}|\Delta\Lambda_l(1)| = A \sum_{s=0}^{M-1} \sum_{n=0}^{N_{s,k}-1} |h_{s,k,n}^i| \tag{22}$$

Proof: Considering W^{-lk} as vectors bisecting unit circles into M equal sectors, the maximum of $|\Delta\Lambda_l(1)|$ is when all the contributing vectors are in the same direction and with maximum amplitude. This happens when $l = M/2$, where only vectors of $\overline{1}$ and $\overline{-1}$ are participating in (17). Using maximum positive coefficients for $\overline{1}$ and minimum negative coefficients for $\overline{-1}$ one ends up to (22).

Corollary 3: If $a_{s,k,n}$'s are zero mean, independent Gaussian random variables, then $|\Delta\Lambda_l(1)|$ and $\angle\Lambda_l(1)$ have Rayleigh and uniform distribution respectively.

Proof: $\Delta\Lambda_l(1)$ can be written as

$$\Delta\Lambda_l(1) = \frac{1}{M} \sum_{k=0}^{M-1} \left(\sum_{s=0}^{M-1} \sum_{n=0}^{N_{s,k}-1} a_{s,k,n} h_{s,k,n}^i \right) \cos\frac{2\pi lk}{M} + \frac{j}{M} \sum_{k=0}^{M-1} \left(\sum_{s=0}^{M-1} \sum_{n=0}^{N_{s,k}-1} a_{s,k,n} h_{s,k,n}^i \right) \sin\frac{2\pi lk}{M} \tag{23}$$

The real and imaginary parts are linear combination of Gaussian random variables, hence they are Gaussian as well. Also they are uncorrelated with respect to each other and the variance of each of them is

$$\sigma_{Re}^2 = \sigma_{Im}^2 = \sigma^2 = \frac{\sigma_a^2 \sum_{s=0}^{M-1} \sum_{n=0}^{N_{s,k}-1} (h_{s,k,n}^i)^2}{2M} \tag{24}$$

Hence, $\rho = |\Delta\Lambda_l(1)|$ is a random variable with the following Rayleigh distribution [4]

$$f_\rho(\rho) = \frac{\rho}{\sigma^2} e^{-\frac{\rho^2}{2\sigma^2}} \qquad \rho \geq 0 \tag{25}$$

and $\theta = \angle\Delta\Lambda_l(1)$ is uniformly distributed as

$$f_\theta(\theta) = \frac{1}{2\pi} \qquad 0 \leq \theta \leq 2\pi \tag{26}$$

Also, using (25) it can be concluded that

$$P\{|\Delta\Lambda_l(1)| \leq \sigma\sqrt{2\log(\frac{1}{1-p})}\} = p \tag{27}$$

Example: Consider $H(z) = (1-z^{-1})^2(1+z^{-1})$, $M = 2$ and $a_{s,k,n}$'s zero mean Gaussian i.i.d. with $\sigma_a = 0.01$. Hence,

$$\overline{H}(z) = \begin{bmatrix} 1-z^{-1} & -1+z^{-1} \\ -z^{-1}+z^{-2} & 1-z^{-1} \end{bmatrix} \tag{28}$$

and $\sum_{s=0}^{M-1} \sum_{n=0}^{N_{s,k}-1} h_{s,k,n}^2 = 4$. After performing a Monte Carlo simulation for 100 times the pdf shown in Fig. 5 is obtained. The theoretical pdf is also depicted on the same figure and shows good agreement. Also, according to corollary 3, with a probability of 99%, $|\Delta\Lambda_l(1)| \leq -28.5dB$. Based on the 100 simulations, $\text{Max}|\Delta\Lambda_l|$ is $-28dB$ while the other 99 values are less than $-28.5dB$ which shows good agreement with theory. In summary, if the modulator's coefficients are mismatched by around 1%, the quantization noise in the vicinity of $f_s/2$ will be attenuated by at least $-28.5dB$ before being aliased back to the band of interest in 99% of times. Finally, the expected value of alias attenuation, $E(|\Delta\Lambda_l(1)|^2)$, is found to be $-33.5dB$ based on simulation and $-37dB$ according to theory. Again, both results are in good agreement with each other.

In summary, any component mismatching will cause certain parts of the spectrum (around $2\pi k/M$, $k = 1, \ldots, M-1$) to be aliased back into the band of interest after going through some attenuation the amount of which is determined by the mismatch ratio (σ_a). To alleviate this effect, the spectrum should be shaped in such a way that it has very little energy around $2\pi k/M$. Two approaches are presented here to serve this purpose for a time-interleaved D/A. In the first approach a post digital filter with transfer function $P(z) = 1 + z^{-1} + \ldots + z^{-(M-1)}$ will generate zeros at $z_k = e^{-j2\pi k/M}$ for $k = 1, \ldots, M-1$. This post digital filter can also be implemented in block form. One problem with this approach is that the output of such a filter is a multi-bit one and hence one requires a multi-bit D/A in the design. The second approach is to include these zeros in the noise transfer function of the modulator directly which in turn increases the complexity of the modulator block and

somewhat degrades SNR. As an example consider a second order noise transfer function $NTF(z) = (1-z^{-1})^2$ and $M = 2$. By modifying it into $NTF_m(z) = (1-z^{-1})^2(1+z^{-1})$, a zero is inserted at $z = -1$, but at the same time the in-band noise would be $6dB$ more powerful than that of the previous case due to DC gain of $1+z^{-1}$. To compensate this extra DC gain of 2, a second zero at $1/2$ is introduced. Finally, the suggested noise transfer function would be $NTF_m(z) = (1-z^{-1})^2(1+z^{-1})(1-z^{-1}/2)$. According to simulation, using the final $NTF_m(z)$ will still cause a $3dB$ loss in SNR in comparison to $NTF(z) = (1-z^{-1})^2$. The authors suspect that increasing the order of the modulator causes the one bit quantizer to be overloaded more often and thus reduces the SNR. Note that the second approach is applicable for a time-interleaved A/D as well.

V. CONCLUSION

Component mismatches in the design of recently reported time-interleaved oversampling converters were discussed and experimental results were given for a second-order time-interleaved D/A modulator. The problem of mismatching was addressed and analytical results were given to estimate the amount of aliasing for a block digital filter, particularly for an FIR structure. Finally, a method was suggested to alleviate the effect of aliasing by reducing the spectrum energy in the vicinity of those parts of spectrum which would be aliased back into the band of interest.

REFERENCES

[1] R. Khoini-Poorfard and D. A. Johns, "Time-interleaved oversampling converters", IEE Electronics Letters, Vol. 29, No. 19, September 1993, pp. 1673-1674.

[2] W. C. Black and D. A. Hodges, "Time interleaved converter arrays," *IEEE Journal of Solid-State Circuits*, Vol. SC-15, No. 6, pp. 1022-1029, December 1980.

[3] P. P. Vaidyanathan, *Multirate systems and filter banks*, Englewood Cliffs, NJ, Prentice Hall, 1993.

[4] A. Papoulis, *Probability, Random variables, and stochastic processes*, 3rd edition, McGraw-Hill, New York, 1991.

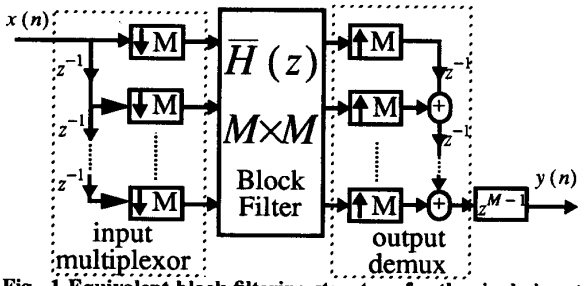

Fig. 1 Equivalent block filtering structure for the single-input single-output transfer-function $H(z)$.

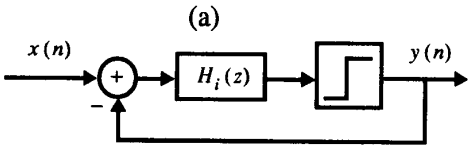

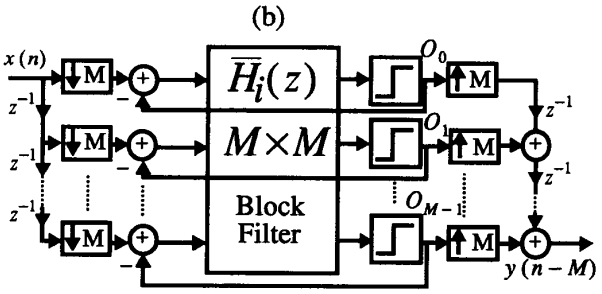

Fig. 2 Interpolative ΔΣ structure. (a) Conventional structure (b) Time-interleaved structure

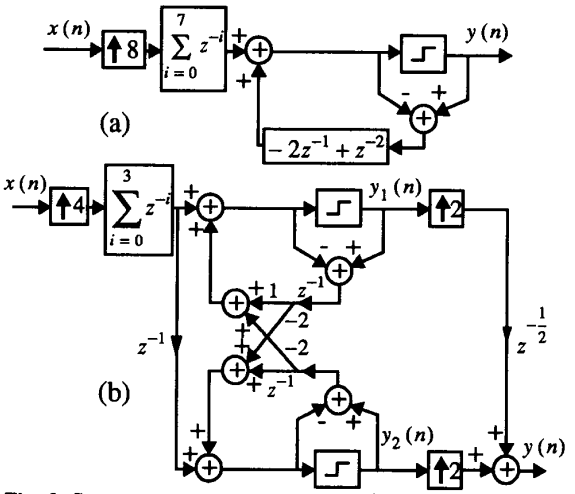

Fig. 3. Second order error-feedback D/A: (a) Conventional, (b) Time-interleaved

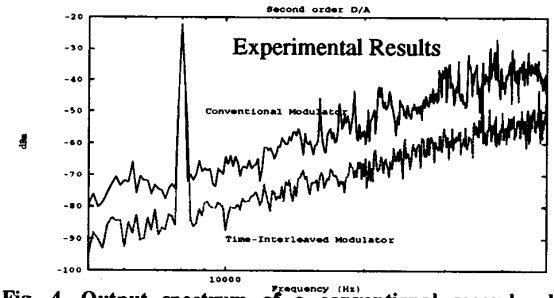

Fig. 4. Output spectrum of a conventional second-order modulator and a time-interleaved one. Both modulators are internally clocked at the same frequency.

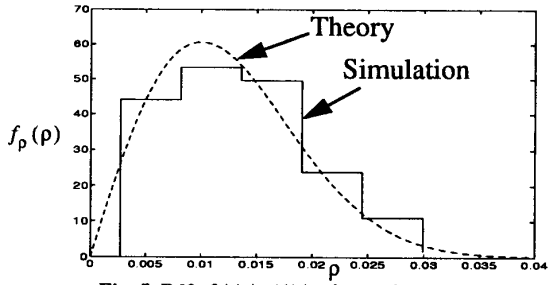

Fig. 5. Pdf of $|\Delta\Lambda_l(1)|$, simulation vs. theory